

# Gamma-ray emission from primordial black hole-neutron star interaction

Oscar del Barco<sup>\*</sup>

*Laboratorio de Óptica, Instituto Universitario de Investigación en Óptica y Nanofísica, Universidad de Murcia, Campus de Espinardo, E-30100, Murcia, Spain*

17 August 2022

## ABSTRACT

The interaction of an asteroid-mass primordial black hole (PBH) with a slowly-rotating neutron star (NS) can lead to detectable gamma-ray emission via modern observatories like Fermi-LAT or e-ASTROGRAM. Depending on the specific PBH relativistic orbit in the NS Schwarzschild spacetime and the relative orientation of this binary system with respect to Earth, the PBH Hawking radiation will show a characteristic temperature profile over time. Essentially, a moderate heating behaviour (or even a progressive and constant cooling phase) is found for the majority of the event, followed by a sudden and dramatic cool-down at the end of the burst. Our theoretical model might provide a means of identification of such hypothetical PBH-NS interactions, based on the distinctive temperature evolution of thermal-like gamma ray bursts (GRBs) described in this article.

**Key words:** gamma-ray bursts – dark matter – black hole - neutron star mergers

## 1 INTRODUCTION

Primordial black holes constitute an hypothetical type of black holes (BHs) formed in the early Universe through gravitational collapse of extremely dense regions (Zeldovich 1967; Hawking 1971; Carr 1974). The study of such ultracompact objects of primitive origin is a subject of continuous research since it is thought that part or the totality of the dark matter (DM) might be formed by PBHs of different masses (Inomata 2017; Bartolo 2019; Belotsky 2019; deLuca 2021). In this regard, a significant part of the dark matter in the Universe range in the  $10^{13} - 10^{14}$  kg,  $10^{17} - 10^{21}$  kg and  $10 - 10^3 M_{\odot}$  window, not excluding lighter PBHs with less contribution to the total amount of DM (Carr 2020, 2021, 2022). It is also evident that these PBH masses are significantly lower than the already evidenced supermassive black holes (Akiyama 2019, 2022).

Specifically, PBHs within the  $10^{13} - 10^{14}$  kg interval are constrained by observations of Galactic center positrons and gamma-rays (Laha 2019, 2020; Dasgupta 2020), while new limitations on spinning and non-spinning PBHs have been reported (Saha 2022). Larger PBHs in the solar-mass range have recently been associated with gravitational wave signals (Kohri 2021) while PBHs smaller than  $10^{12}$  kg would have presently evaporated due to its Hawking emission (Ackermann 2018). Current observations reported plausible PBH detection via their Hawking radiation in the mass range  $8 \times 10^{11} - 10^{13}$  kg (Wang 2021). Moreover, ultra-light PBHs with masses less than  $10^6$  kg (which would have evaporated before big-bang nucleosynthesis) might have been predominant in the early Universe (Papanikolaou 2021).

Among all of these different mass windows, the so-called asteroid-mass PBHs (AMPBHs) have drawn increasing attention. Some authors set the mass limit of these light BHs within the mass interval  $7 \times 10^{13} - 8 \times 10^{18}$  kg (Montero-Camacho 2019) whereas other researchers suggest PBHs with masses less than  $2 \times 10^{19}$  kg as a

reasonable definition for AMPBHs (Miller 2022). In any case, these asteroid-mass PBHs have lifetimes ranging from hundreds to several million times the age of the Universe and constitute a serious candidate for the cosmological dark matter (Coogan 2021). New constraints on this asteroid-mass window have been lately reported (Smyth 2020; Miller 2022), being a matter of subsequent research via future gamma ray telescopes such as the upcoming AMEGO (Ray 2021).

Recently, a plausible PBH origin for thermal GRBs was stated, where an atomic-sized PBH described a radial fall onto a massive black hole (Barco 2021, 2022). As a result, the numerical calculations for the PBH Hawking emission were consistent with thermal-like gamma ray bursts (GRBs) in the MeV domain. However, this study considered a quite restrictive interaction between both black holes, that is, a plunging orbit where the PBH is being captured by its massive companion. No other possible relativistic orbits were analyzed in this paper and a detailed discussion of the rate of occurrence of such events was not provided.

In the present article, the above-mentioned astrophysical scenario and the related theoretical model are both updated to take into account a more general PBH interaction event. Indeed, an asteroid-mass PBH experiences a close approach to a slowly-rotating neutron star (Yazadjiev 2016; Motahar 2017; Boumaza 2021) well approximated by a Schwarzschild spacetime. Two different relativistic orbits are studied in our model, that is, a plunge case (where the PBH orbit intercepts the NS surface) and a scattering event around the NS, both with characteristic and recognizable Hawking emission profiles. Moreover, a complete analysis of the rate of occurrence of both events (following Capela (2013) formalism) is carried out.

The paper is organized as follows. In section 2 we describe our astrophysical scenario and develop the theoretical framework to calculate the PBH relativistic orbits and its fluence spectrum  $\nu S_{\nu}$  during the whole event. A detailed numerical study concerning the PBH plunge and scattering orbits and its associated Hawking temperature evolution are performed in section 3. A moderate heating behaviour

<sup>\*</sup> E-mail: obn@um.es

(or a progressive and constant cooling, depending on the PBH orbit) is found for the majority of the event, followed by a sudden and dramatic cool-down at the end of the burst. The gamma-ray emission due to the PBH Hawking radiation might be detected via modern observatories like Fermi-LAT or e-ASTROGRAM. For completeness, the rate of occurrence of such PBH-NS interactions is fully analyzed in section 4. Finally, we summarize our results in section 5.

## 2 THEORETICAL BASIS

Let us consider the astrophysical scenario depicted in Fig. 1. Here, an AMPBH of mass  $M_P$  describes a relativistic orbit around an isolated slowly-rotating NS of radius  $R_{NS}$ , at distance  $d_s$  from Earth. It is also assumed that our NS does not accrete matter from any stellar material, with such a low temperature so that its proper thermal emission is practically negligible (Pearson 2018, 2019; Fantina 2020).

According to Fig. 1, when the PBH is located at position (1) (within the so-called non-detection area), its Hawking emission lies below the typical sensibility of modern observatories and, consequently, it cannot be initially detected. Once the PBH approaches the NS and its velocity component is pointing directly towards the Earth (as in position (2)), its Hawking radiation is significantly Lorentz-boosted and might be measured in the MeV range. The parameter  $\theta_e$  corresponds to the angle between the radial coordinate  $\hat{r}$  and the photon emission direction (supposed along the Earth's line of sight, ELS). As the PBH goes around the NS (in the case of a scattering orbit), the velocity component is now opposite to the ELS so a deboosting effect occurs (please, see position (3) in Fig. 1). In this situation, the Hawking emission drops below the gamma-ray observatories sensibility and enters again the non-detection area.

Under these premises, the NS spacetime can be properly modelled by the Schwarzschild line element

$$ds^2 = -f(r)dt^2 + f(r)^{-1}dr^2 + r^2(d\theta^2 + \sin^2\theta d\phi^2), \quad (1)$$

where  $r$  indicates the radial coordinate of the PBH (our emitter),  $f(r) = 1 - 2M_{NS}/r$  and  $M_{NS}$  stands for the mass of our NS. Trivially, for a distant observer placed at  $r_{obs}$  (for example, an observatory on Earth), the parameter  $f(r_{obs}) \simeq 1$ .

Throughout the article, the geometrized system of units ( $c = G = 1$ ) is adopted, except for radiometric magnitudes where the S.I. system of units is considered. We also assume that the PBH motion is confined at the equatorial plane  $\theta = \pi/2$  with conserved specific energy  $E_s$  and positive specific angular momentum  $L_s$ . Both parameters will determine the specific PBH orbit, as will be briefly discussed.

On the other hand, the kinematic component of the time dilation  $\gamma$  can be expressed as (Hartle 2003)

$$\gamma = (1 - \beta^2)^{-1/2} = \frac{E_s}{\gamma_G}, \quad (2)$$

where  $\beta$  is the velocity of the PBH and  $\gamma_G = \sqrt{f(r)}/\sqrt{f(r_{obs})} \simeq \sqrt{f(r)}$ . We can also write the coordinate time  $t$  (for a distant observer) and the azimuthal angle  $\phi$  as a function of the PBH radial coordinate  $r$  via the following differential equations (Hartle 2003)

$$dt = \frac{E_s}{f(r)} \left[ E_s^2 - f(r) \left( 1 + \frac{L_s^2}{r^2} \right) \right]^{-1/2} dr, \quad (3)$$

and

$$d\phi = \frac{1}{r^2} \left[ \frac{1}{b^2} - f(r) \left( \frac{1}{L_s^2} + \frac{1}{r^2} \right) \right]^{-1/2} dr, \quad (4)$$

where  $b = L_s/E_s$ . After numerical resolution of both expressions (3)

and (4), the event duration (from the point of view of an observer on Earth) and the PBH specific orbit will be respectively derived.

Furthermore, the PBH Hawking temperature as measured by the emitter ( $T'_P$ ) and a distant observer ( $T_P$ ) are related via the redshift (blueshift) factor  $\alpha$  (McMaken 2022)

$$T_P = \alpha T'_P = \gamma_G \left( \gamma \pm \cos\theta_e \sqrt{\gamma^2 - \left( 1 + \frac{L_s^2}{r^2} \right) \mp \frac{L_s}{r} \sin\theta_e} \right)^{-1} T'_P, \quad (5)$$

where the upper (bottom) signs stand for an infalling (outgoing) relativistic orbit (such as the scattering case described in Fig. 1) and  $T'_P$  can be well approximated by (Hawking 1974, 1975)

$$T'_P = (6.169 \times 10^{-8}) \frac{M_\odot}{M_P}, \quad (6)$$

where the temperature is expressed in Kelvins. One notices that the PBH Hawking temperature  $T_P$  depends on its mass (that is, lighter PBHs would be at higher temperature), the constants of motion  $E_s$  and  $L_s$  (i.e., the specific PBH orbit in the NS spacetime) and the photon emission direction  $\theta_e$  (or, equivalently, the position of the PBH in its relativistic orbit).

Considering a slowly-rotating PBH, it is thus appropriate to model the Hawking emission as a blackbody radiator (Murata 2006; Barco 2021), so the fluence spectrum  $\nu S_\nu$  for a static observer on Earth can be expressed as (S.I. units)

$$\nu S_\nu = \frac{2\pi h \nu^4 \Omega}{c^2} \left( \exp \left[ \frac{h\nu}{kT_P} \right] - 1 \right)^{-1}, \quad (7)$$

and  $\Omega = \pi r_D^2/d_s^2$  is the solid angle subtended by a point source for a detector of radius  $r_D$  (which, in turn, is proportional to the effective area  $A_{eff}$  of our gamma-ray telescope). As discussed in the next section, our astrophysical scenario predicts a fluence spectrum  $\nu S_\nu$  of finite duration lying within the MeV range.

## 3 NUMERICAL RESULTS

In this section, a complete numerical analysis of the PBH relativistic orbits and the associated Hawking emission (in connection with thermal-like GRBs) is carried out.

Firstly, let us analyze the different PBH scenarios allowed in our model within the theoretical framework of the NS Schwarzschild spacetime. Without loss of generality, the mass of our PBH will be  $10^{12}$  kg throughout the article (that is, in the range of the aforementioned asteroid-mass interval (Miller 2022)). As already stated, the specific PBH orbit depends on the conserved magnitudes  $E_s$  and  $L_s$  via the effective potential  $V_{eff}$  (Hartle 2003)

$$V_{eff}(r) = \frac{1}{2} \left[ f(r) \left( 1 + \frac{L_s^2}{r^2} \right) - 1 \right]. \quad (8)$$

When  $(L_s/M_{NS}) > \sqrt{12}$ , the effective potential has one maximum and one minimum: this will be the situation considered in our model. Moreover, the specific orbit depends on the relationship between the parameter  $\epsilon = (E_s^2 - 1)/2$  and  $V_{eff}$ . If  $\epsilon > V_{eff}^{(max)}$ , the PBH describes a plunge orbit onto the NS (and, eventually, it might be captured by the latter, as remarked in section 4). When  $0 < \epsilon < V_{eff}^{(max)}$ , a scattering orbit occurs where the PBH comes in from infinity, orbits the NS and moves out to infinity again (as illustrated in Fig. 1).

The effective potential  $V_{eff}$  is calculated via equation (8) and represented in Fig. 2 for a typical neutron star of mass  $M_{NS} = 1.4M_\odot$  and radius  $R_{NS} = 1.2 \times 10^4$  m. The selected value for the PBH specific angular momentum was  $L_s = 9 \times 10^3$  m. With this choice, the

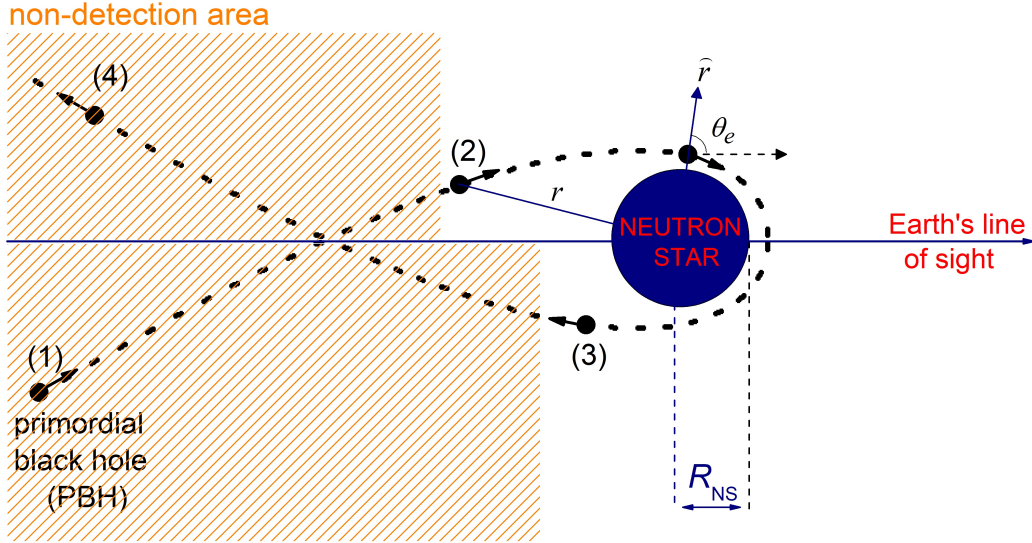


**Figure 1.** Schematic representation of our astrophysical scenario: an AMPBH describes a relativistic orbit around an isolated slowly-rotating NS. When the PBH is located at the shadowed region (that is, the so-called non-detection area), its Hawking radiation is too dim to be detected via modern gamma-ray observatories. As the PBH approaches the NS, its Hawking emission is firstly Lorentz-boosted (please, see position (2)) and then gradually deboosted (position (3)) when it completes its orbit around the compact object (as in the case of a typical scattering orbit). The parameter  $\theta_e$  corresponds to the angle between the radial coordinate  $\hat{r}$  and the photon emission direction (supposed along the Earth's line of sight).

NS effective potential presents one maximum and one minimum, though this prerequisite is not essential for our model (as in the case when  $(L_s/M_{\text{NS}}) < \sqrt{12}$  where only plunge orbits are allowed). Two different values of the parameter  $\epsilon$  are shown in Fig. 2, each representing a characteristic PBH orbit: a plunge event for  $\epsilon_p = 0.105$ , corresponding to a PBH specific energy  $E_s = 1.1$  and a velocity at infinity of  $0.41c$ , and a scattering orbit for  $\epsilon_s = 0.0$ , where the PBH exhibits a free fall from infinity. In this case, the intercept of  $\epsilon$  with the effective potential curve gives us the minimum approach of the PBH to the NS (that is,  $r_{\text{min}} = 1.38 \times 10^4$  m).

In this context, the specific shape of each PBH orbit (obtained via numerical resolution of equation (4)) is represented in Fig. 3, where the radial  $r$  and azimuthal  $\phi$  coordinates (last one in degrees) are plotted as polar diagrams in the equatorial plane  $\theta = \pi/2$ . Top panel depicts two identical AMPBHs describing different plunging orbits (in relation to their relative orientation with respect to the ELS, and denoted as  $\text{PBH}_{(1)}$  and  $\text{PBH}_{(2)}$ , respectively), while bottom panel shows two scattering events for the same astrophysical scenario. In both cases, the same parameters as in Fig. 2 have been selected. In connection with Fig. 1, the infalling PBH approaching the NS from infinity is not initially detected (due to its faint Hawking emission). Depending on its particular orbit, the PBH Hawking radiation will be rather different and recognizable, as briefly discussed.

In Fig. 4, the PBH Hawking temperature  $T_p$  is illustrated as a function of the radial coordinate  $r$  for each particular orbit in Fig. 3. All our numerical calculations have been performed via equation (5). For both plunge and scattering events, there exists a minimum value of the PBH Hawking temperature  $T_p^{(\text{min})}$  (i.e., the dashed horizontal lines in top and bottom panels in Fig. 4) below which the fluence spectrum  $\nu S_\nu$  is too dim to be detected by modern observatories. It should be also pointed out that this temperature threshold strongly depends on the PBH mass, its distance to the Earth (or, equivalently, the solid angle subtended by such point source) and the sensitivity of the gamma-ray telescopes. Once our PBH is close enough to the NS, its Hawking temperature exceeds  $T_p^{(\text{min})}$  and its emission is likely

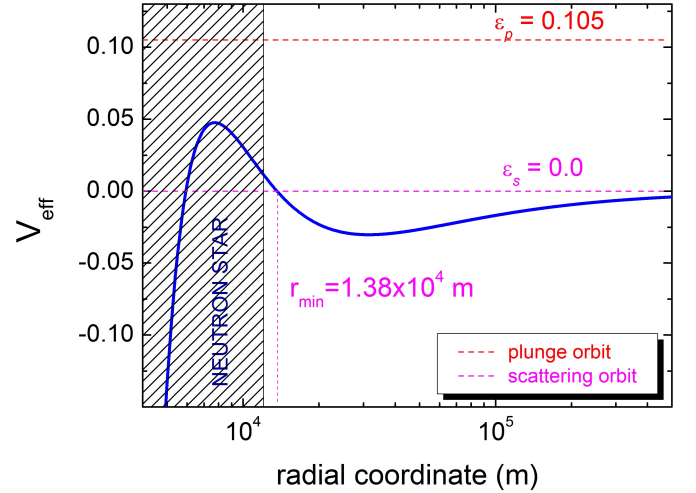


**Figure 2.** The effective potential  $V_{\text{eff}}$  versus the radial coordinate  $r$  (calculated via equation (8)) for a NS of mass  $M_{\text{NS}} = 1.4M_\odot$  and radius  $R_{\text{NS}} = 1.2 \times 10^4$  m (considering that the slowly-rotating NS spacetime is well-approximated by the Schwarzschild metric). The selected value for the PBH specific angular momentum was  $L_s = 9 \times 10^3$  m, so  $V_{\text{eff}}$  presents one maximum and one minimum. Two different values of the parameter  $\epsilon$  are shown, each representing a characteristic PBH orbit: a plunge event for  $\epsilon_p = 0.105$ , corresponding to a PBH specific energy  $E_s = 1.1$  and a velocity at infinity of  $0.41c$ , and a scattering orbit for  $\epsilon_s = 0.0$ , where the PBH exhibits a free fall from infinity. For the scattering orbit, the minimum approach of the PBH to the NS resulted to be  $r_{\text{min}} = 1.38 \times 10^4$  m.

to be measured: this is the beginning of the thermal GRB of finite duration (and calculated after numerical resolution of differential equation (3), as shortly presented). This prompt gamma-ray emission is concluded when  $T_p$  drops below the threshold temperature  $T_p^{(\text{min})}$

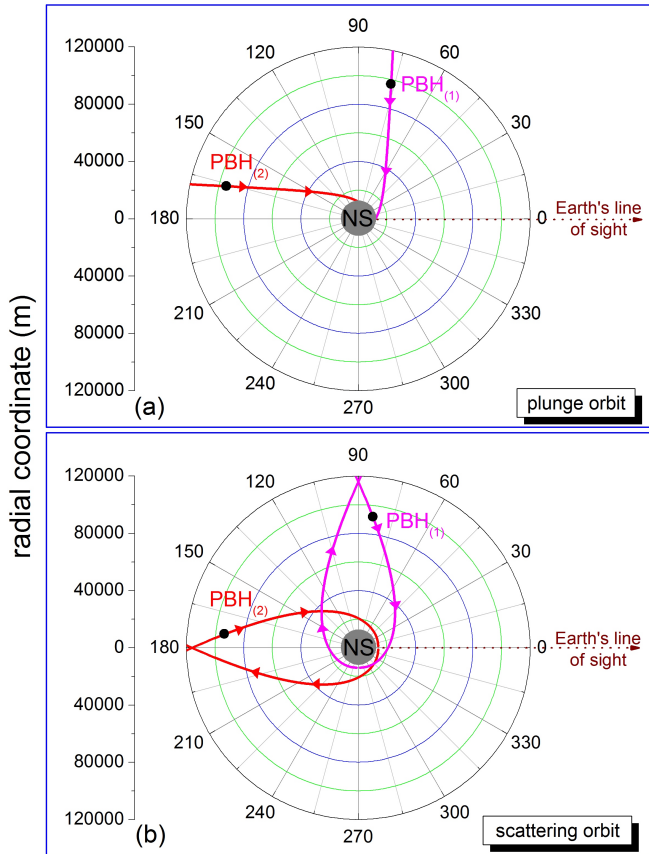


**Figure 3.** Polar diagrams for the radial  $r$  and azimuthal  $\phi$  coordinates (last one in degrees) obtained via numerical resolution of equation (4). Two different AMPBH scenarios are considered (same parameters as in Fig. 2): (a) plunge and (b) scattering orbits. For each panel, two different relative orientations of the PBH with respect to the ELS are also shown (and denoted as  $\text{PBH}_{(1)}$  and  $\text{PBH}_{(2)}$ , respectively).

again, a process which is highly dependent on the PBH relativistic orbit. Indeed, the  $\text{PBH}_{(2)}$  orbit in Fig. 4(a) will produce a detectable GRB of 0.9 s, while the plunge orbit for  $\text{PBH}_{(1)}$  will remain unnoticed for current observatories. On the other hand, both scattering orbits in Fig. 4(b) will be experienced as thermal-like GRBs of specific duration (about 35 s for  $\text{PBH}_{(1)}$ ).

It can be noticed that the PBH Hawking temperature presents an initial heating behaviour (due to the Lorentz-boosting of  $T_P$  when the PBH velocity component is directed towards the ELS), followed by a dramatic cool-down, when the PBH velocity component is opposite to the Earth's line of sight (and a Lorentz-deboosting process occurs). This heating evolution is more pronounced (and eventually reaching a well-defined maximum temperature) for relativistic orbits where the PBH velocity component is mainly maintained towards us during practically the whole event (please, see again the  $\text{PBH}_{(2)}$  cases in Fig. 4). In the opposite scenarios (as in the  $\text{PBH}_{(1)}$  events), there exists a moderate heating process (such as the scattering orbit in bottom panel) or even a progressive and constant cooling, as in the plunge case in Fig. 4(a). The latter situation is more consistent with already reported cooling behaviour of thermal GRBs (Ryde 1999, 2004; Barco 2021, 2022). It should be added that, as the PBH travels away from the NS in the scattering case, its Hawking temperature (as calculated via equation (5), under the appropriate choice of signs)

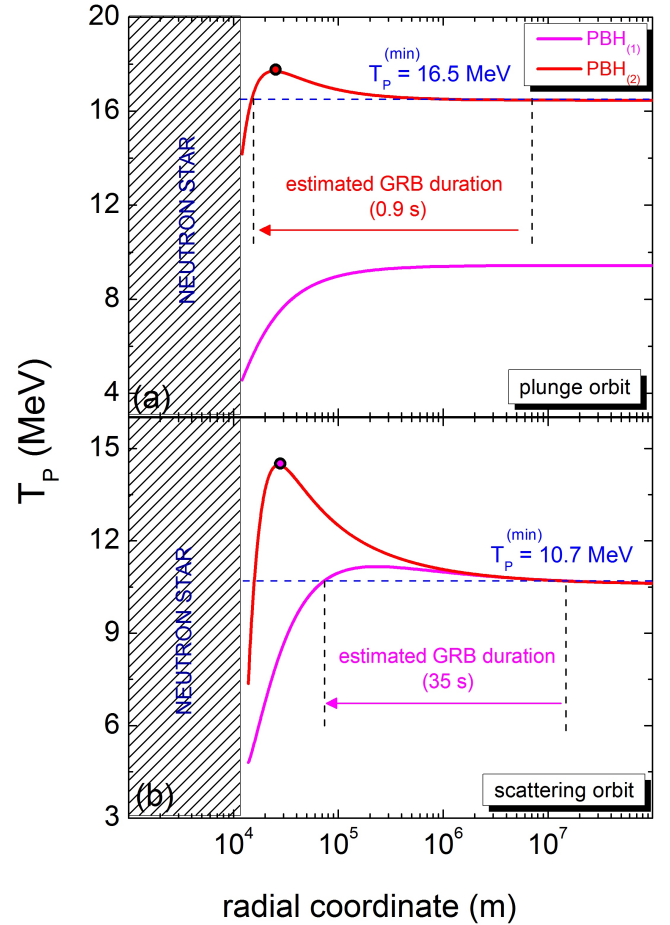


**Figure 4.** PBH Hawking temperature  $T_P$  versus the radial coordinate  $r$  for each specific orbit, calculated numerically via equation (5) (same parameters as in Fig. 3). The threshold value of the PBH Hawking temperature  $T_P^{(\min)}$  detectable by modern observatories on Earth is represented as dashed horizontal lines in both panels: (a) plunge orbits, where the  $\text{PBH}_{(2)}$  event might be measured as a thermal-like GRB of 0.9 s duration and (b) scattering cases, with an estimated time span of 35 s for  $\text{PBH}_{(1)}$ .

continues its fall and never goes above the threshold temperature  $T_P^{(\min)}$ . Provided the irrelevance of such results to the detectability of scattering events, these computational values have not been included in Fig. 4(b).

The corresponding temporal evolution of the PBH Hawking temperature  $T_P$  is shown in Fig. 5 (via numerical resolution of equation (3) and same parameters as in Fig. 4). For the  $\text{PBH}_{(2)}$  plunge case (upper panel) and the  $\text{PBH}_{(1)}$  scattering event (bottom panel), a moderate heating behaviour is obtained followed by a dramatic temperature drop of millisecond duration, as depicted in the insets (where the abscissa axis represents the coordinate time  $t$ , once the estimated GRB duration  $\Delta_{\text{GRB}}$  is subtracted). This is probably the new signature reported in this article, where the cooling phase is much too steep compared to the heating one.

In relation to the fluence spectrum  $\nu S_\nu$ , plausibly measurable by modern gamma-ray stations, Fig. 6 shows this magnitude for the  $\text{PBH}_{(2)}$  events and calculated via equation (7) (please, see again Figs. 3 and 4). It can be observed a typical Planckian-like distribution for  $\nu S_\nu$ , in accordance with the PBH thermal emission. For the

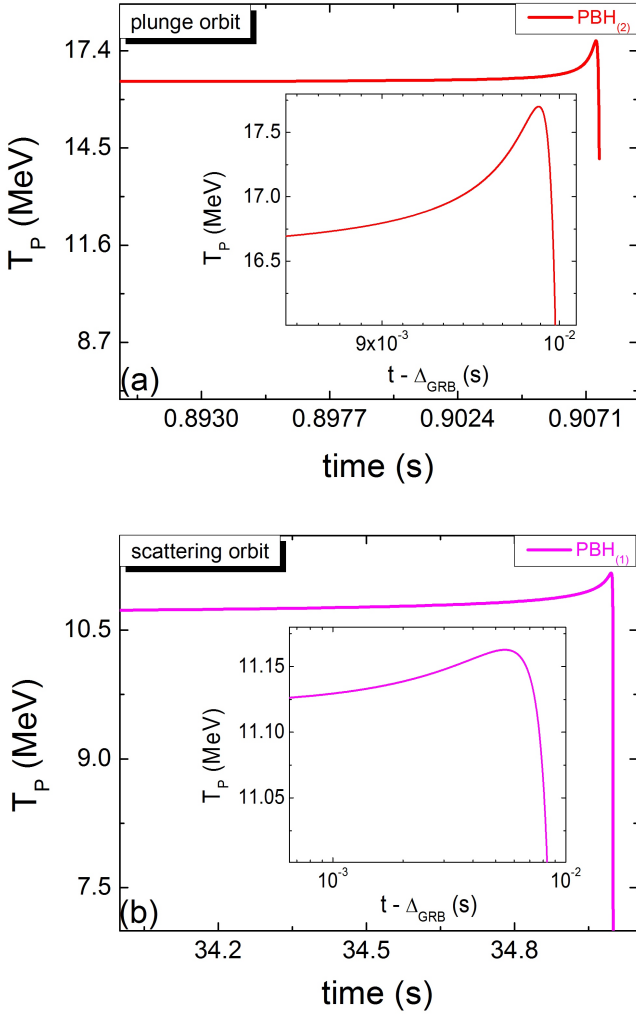


**Figure 5.** PBH Hawking temperature  $T_P$  as a function of the observer's coordinate time  $t$ , numerically calculated via equation (3) (same parameters as in Fig. 4). For a better visualization of the rapid cooling phase in both panels, two insets have been included where the horizontal axis describes the coordinate time  $t$ , once the estimated GRB duration  $\Delta_{\text{GRB}}$  is subtracted.

plunge orbit case (top panel), the fluence spectrum corresponding to a minimum Hawking temperature of 16.5 MeV practically reaches the sensitivity of the Fermi-LAT observatory (deAngelis 2018). For this calculation, an estimated distance to Earth of 4.2 Gparsec and an effective area  $A_{\text{eff}} = 10^4 \text{ cm}^2$  for the Fermi-LAT (Coogan 2021) have been considered. Furthermore, the PBH fluence spectrum  $\nu S_\nu$  for the maximum Hawking temperature 17.7 MeV (i.e., the red dot shown in Fig. 4(a)) is also represented, where now  $\nu S_\nu$  is well above the Fermi-LAT sensitivity.

In Fig. 6(b), the scattering orbit event is depicted for a PBH-NS system at 2.3 Gparsec from Earth. One notices that the minimum fluence spectrum (associated with the threshold temperature  $T_P^{(\text{min})} = 10.7 \text{ MeV}$ , please see again Fig. 4(b)) is of the order of the e-ASTROGRAM observatory sensibility (deAngelis 2018), with an estimated effective area  $A_{\text{eff}} = 2 \times 10^3 \text{ cm}^2$  in the MeV domain (Coogan 2021). The maximum value for  $\nu S_\nu$  (corresponding to a PBH temperature of 14.5 MeV, as illustrated in Fig. 4(b) with a red dot) peaks above the Fermi-LAT sensitivity, being detectable at

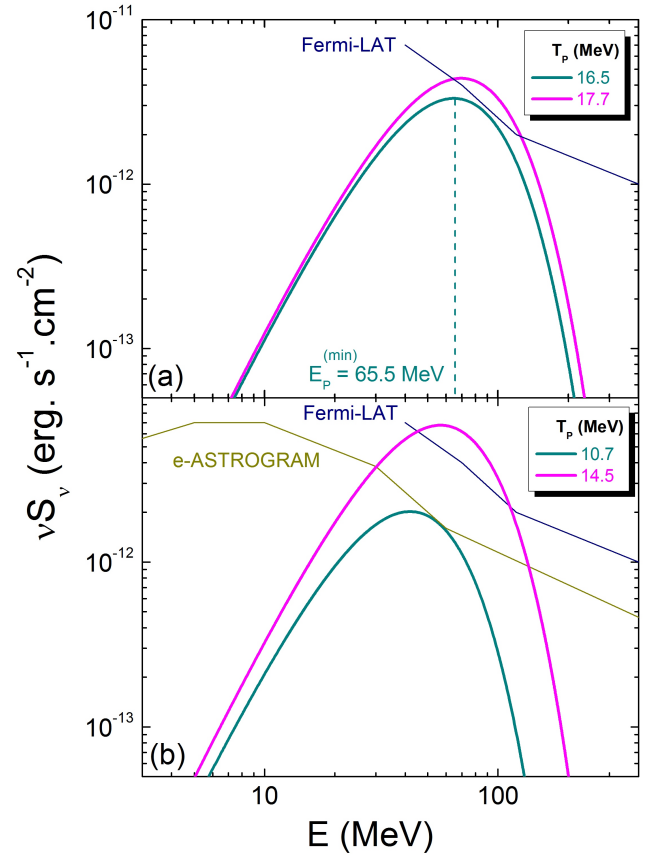


**Figure 6.** Fluence spectrum  $\nu S_\nu$  for the minimum and maximum PBH Hawking temperatures (same parameters as in Figs. 3 and 4) for the PBH<sub>(2)</sub> events. Our numerical results were calculated via equation (7) for (a) plunge and (b) scattering orbits. It can be observed a typical Planckian-like distribution for  $\nu S_\nu$ , in accordance with the PBH thermal emission. As an indicative manner, the sensitivities of the e-ASTROGRAM and Fermi-LAT telescopes are shown.

the final stage of the burst (just before the cooling phase), via such modern observatories.

At the same time, it should be recalled that our slowly-rotating NS does not possess an accretion disk (Pearson 2018, 2019; Fantina 2020), unlike other younger and more active NSs. The presence of such structure in our binary astrophysical scenario might modify our previous fluence calculations, due to the thermal emission of this accretion disk. Additionally, as previously commented, our isolated NS has cooled down sufficiently so that its proper thermal emission is negligible.

To complete this section, it is worth asking how frequent are such PBH-NS interactions, in order to be detectable by gamma-ray observatories. We will try to give a satisfactory response on this topic in the next section.

#### 4 RATE OF OCCURRENCE ANALYSIS

Let us now examine the rate of occurrence  $\mathcal{F}$  of such PBH-NS scenarios, including the already studied plunge and scattering cases. Such astrophysical events have been earlier reported in the literature where (in a more restrictive situation), a PBH is captured by a neutron star (Capela 2013; Pani 2014). In this way, it is a reasonable

assumption that the PBH-NS events leading to the above-mentioned GRBs should be of extragalactic nature (otherwise, nearby galaxies would be a remarkable source of brighter gamma ray transients, a possibility that must be discarded).

Following the formalism by Kouvaris (2008) and Capela (2013), the parameter  $\mathcal{F}$  is derived by integrating a Maxwellian dark matter distribution, with velocity dispersion  $\bar{v}$ , over the  $E_s$  and  $L_s$  space with well-defined integration limits. Within this theoretical framework, a PBH is captured and becomes gravitationally bound when it loses its initial energy due to the accretion of star's material. Nevertheless, we would not adopt such limiting situation: it would be enough for us to consider that the PBH orbit intercepts the NS surface (as in the case of a plunge event) or that the PBH passes close enough to the NS (for a scattering scenario).

Accordingly, the parameter  $\mathcal{F}$  for a NS of radius  $R_{\text{NS}}$  can be written as (Capela 2013)

$$\mathcal{F} = \sqrt{6\pi} \frac{\Omega_{\text{PBH}}}{\Omega_{\text{DM}}} \frac{\rho_{\text{DM}}}{M_{\text{P}}} \frac{R_{\text{NS}} R_s}{\bar{v} f(R_{\text{NS}})}, \quad (9)$$

where  $\Omega_{\text{PBH}}/\Omega_{\text{DM}}$  is the fraction of PBHs to dark matter,  $\rho_{\text{DM}}$  the local DM density and  $R_s = 2M_{\text{NS}}$  the Schwarzschild radius of the NS. Assuming that the currently estimated DM density ranges from low density regions (where  $\rho_{\text{DM}} \approx 0.5 \text{ GeV.cm}^{-3}$  at the edge of a galaxy) to high values around  $840 \text{ GeV.cm}^{-3}$  at the center of a standard galaxy (Read 2014; Sofue 2020; Chang 2021), a velocity dispersion  $\bar{v} = 7 \times 10^3 \text{ m.s}^{-1}$  and typical NS parameters (i.e.,  $R_{\text{NS}} = 1.2 \times 10^4 \text{ m}$  and  $M_{\text{NS}} = 1.4M_{\odot}$ ), the parameter  $\mathcal{F}$  for an AMPBH of  $10^{12} \text{ kg}$  describing a plunge orbit (and calculated via equation (9)) should be of  $10^{-3} \text{ yr}^{-1}$ . Considering a fraction of dark matter in the form of asteroid-mass PBHs as  $\Omega_{\text{PBH}}/\Omega_{\text{DM}} \approx 10^{-7}$  (Bartolo 2019; deLuca 2021), the rate of occurrence for a single PBH plunge event corresponds to  $\mathcal{F} \approx 10^{-10} \text{ yr}^{-1}$ .

Taking into account an estimated number of  $10^8$  NSs in a galaxy similar to the Milky Way (Sartore 2010; Cordes 2016) and a specific area of the Universe with  $10^3$  galaxies at distances greater than 1 Gparsec from Earth (among  $10^{11}$  galaxies in the observable Universe, as reported by Conselice (2006, 2016); Lauer (2021)), the number of such AMPBH plunge events that might occur at about  $10^3$  distant galaxies should be roughly 12 events per year (assuming an mean value of  $\rho_{\text{DM}} \approx 5 \text{ GeV.cm}^{-3}$  in our calculations). For the scattering case, the rate of occurrence  $\mathcal{F}$  is of the order of 19 events per year (where now the NS radius has been expanded to include such orbits, concretely  $R_{\text{NS}} = 2.4 \times 10^4 \text{ m}$ ).

It is also worth recalling that many of these PBH-NS interactions would not give rise to observable GRBs, mainly due to the small range of successful orientations of our binary system. Moreover, the differences in PBH concentration and DM densities in the Universe (excluding young NSs in the galaxies) could be another limiting factor. Despite the difficulty of finding PBH-NS interactions leading to detectable GRBs (and consistent with our theoretical predictions), those astrophysical scenarios should not be discarded, as already discussed in this section.

## 5 CONCLUSIONS

Summarizing, an astrophysical scenario where an asteroid-mass PBH undergoes a scattering or a plunge orbit towards a slowly-rotating NS can lead to detectable gamma-ray emission, via modern observatories like Fermi-LAT or e-ASTROGRAM. As widely studied in the previous sections, the PBH Hawking radiation shows a well-defined and characteristic temperature profile over time, depending on the

specific PBH event in the NS Schwarzschild spacetime. Related to this, the PBH stable circular orbit (that is, when the parameter  $\epsilon$  equals the minimum value of  $V_{\text{eff}}$ , please see again Fig. 2) has not been discussed in our model. In this hypothetical scenario, a periodic thermal GRB of short duration should be measured, in addition to the earlier described signatures in section 3.

No afterglows are expected for the scattering case, where our PBH goes around the NS and moves away again to infinity (that is, a dark GRB would occur (Fynbo 2001; Jakobsson 2004; Melandri 2012)). Nonetheless, subsequent thermal emission at longer wavelengths (i.e., afterglows within the X-ray or ultraviolet domain) might happen for a plunge event due to the accretion of heated stellar material, once the PBH is trapped by the NS. This accretion mechanism should be more efficient for more massive incoming primordial black holes (such as planetary-mass PBHs) where their event horizon is much greater than the size of an atom: let us recall that the size of an AMPBH (like the one considered in our work) is of the order of an atomic nucleus, roughly  $10^{-15} \text{ m}$ .

As commented in section 4, the rate of occurrence of these PBH-NS interactions (within a specific region of the Universe, covering  $10^3$  galaxies at distances greater than 1 Gparsec from Earth) should be of about 12 or 19 events per year, depending on the plunge or scattering case, respectively. However, all of these events would not produce detectable GRBs, mainly due to the difficulties in the correct alignment of the binary system (that is, only a small range of orientations in our theoretical model could successfully generate such measurable signatures). Moreover, as previously commented, the interaction events resulting in detectable thermal-like GRBs would occur at cosmological distances (that is, when such asteroid-mass PBHs were more abundant than presently), constraining thus the number of PBH-NS plausible scenarios. It can also be expected that future gamma-ray observatories with improved sensitivities might be able to detect such GRBs of primordial black hole origin.

On the other hand, similar results to those detailed in this article are expected if we consider a stellar-mass black hole as the massive central object, instead of a NS. In this context, the asteroid-mass PBH could get through the BH photon sphere and, as a consequence, the cool-down process might be more pronounced and accelerated (Barco 2022).

In conclusion, our theoretical model might provide a way of identifying such feasible PBH-NS interactions, based on the specific temperature profile of the before-mentioned thermal-like GRBs.

## ACKNOWLEDGEMENTS

The author gratefully acknowledges the anonymous reviewer for valuable assistance throughout the refereeing process. O. del Barco warmly acknowledges F. J. Ávila for helpful discussions on neutron star evolution and thanks research support from University of Zaragoza-Fundación Ibercaja (project number JIUZ-2021-CIE-01) and Fundación Séneca - Agencia de Ciencia y Tecnología de la Región de Murcia (19897/GERM/15).

## DATA AVAILABILITY

Provided the theoretical nature of this paper, all data and numerical results generated or analysed during this study are included in this article (and based on the references therein). All the numerical calculations have been carried out on the basis of a Fortran 90 compiler.

## REFERENCES

- Ackermann M., et al., 2018, *ApJ*, 857, 49
- Barco O., 2021, *MNRAS*, 506, 806
- Barco O., 2022, *MNRAS*, 512, 2925
- Bartolo N., De Luca V., Franciolini G., Peloso M., Racco D., Riotto A., 2019, *Phys. Rev. D*, 99, 103521
- Belotsky K. M., et al., 2019, *Eur. Phys. J. C*, 79, 246
- Boumaza H., 2021, *Eur. Phys. J. C*, 81, 448
- Capela F., Pshirkov M., Tinyakov P., 2013, *Phys. Rev. D*, 87, 123524
- Carr B. J., Hawking S. W., 1974, *MNRAS*, 168, 399
- Carr B., Kühnel F., 2020, *Annu. Rev. Nucl. Part. Sci.*, 70, 355
- Carr B., Kohri K., Sendouda Y., Yokoyama J., 2021, *Rep. Prog. Phys.*, 84, 116902
- Carr B., Kühnel F., 2022, *SciPosts Phys. Lect. Notes*, p. 48
- Chang L. J., Necib L., 2021, *MNRAS*, 507, 4715
- Conselice C. J., 2006, *MNRAS*, 373, 1389
- Conselice C. J., Wilkinson A., Duncan K., Mortlock A., 2016, *ApJ*, 830, 83
- Coogan A., Morrison L., Profumo S., 2021, *Phys. Rev. Lett.*, 126, 171101
- Cordes J. M., Wasserman I., 2016, *MNRAS*, 457, 232
- Dasgupta B., Laha R., Ray A., 2020, *Phys. Rev. Lett.*, 125, 101101
- De Angelis A., et al., 2018, *J. High Energy Astrophys.*, 19, 1
- De Luca V., Franciolini G., Riotto A., 2021, *Phys. Rev. Lett.*, 126, 041303
- Event Horizon Telescope Collaboration et al., 2019, *ApJ*, 875, L1
- Event Horizon Telescope Collaboration et al., 2022, *ApJ*, 930, L12
- Fantina A. F., De Ridder S., Chamel N., Gulminelli F., 2020, *A&A*, 633, A149
- Fynbo J. U., et al., 2001, *A&A*, 369, 373
- Hartle J. B., 2003, *Gravity : an introduction to Einstein's general relativity*
- Hawking S. W., 1971, *MNRAS*, 152, 75
- Hawking S. W., 1974, *Nature*, 248, 30
- Hawking S. W., 1975, *Commun. Math. Phys.*, 43, 199
- Inomata K., Kawasaki M., Mukaida K., Tada Y., Yanagida T. T., 2017, *Phys. Rev. D*, 96, 043504
- Jakobsson P., Hjorth J., Fynbo J. P. U., Watson D., Pedersen K., Björnsson G., Gorosabel J., 2004, *ApJ*, 617, L21
- Kohri K., Terada T., 2021, *Phys. Lett. B*, 813, 136040
- Kouvaris C., 2008, *Phys. Rev. D*, 77, 023006
- Laha R., 2019, *Phys. Rev. Lett.*, 123, 251101
- Laha R., Muñoz J. B., Slatyer T. R., 2020, *Phys. Rev. D*, 101, 123514
- Lauer T. R., et al., 2021, *ApJ*, 906, 77
- McMaken T., 2022, *MNRAS*, 511, 1218
- Melandri A., et al., 2012, *MNRAS*, 421, 1265
- Miller A. L., Aggarwal N., Clesse S., De Lillo F., 2022, *Phys. Rev. D*, 105, 062008
- Montero-Camacho P., Fang X., Vasquez G., Silva M., Hirata C. M., 2019, *J. Cosmology Astropart. Phys.*, 2019, 031
- Motahar Z. A., Blázquez-Salcedo J. L., Kleihaus B., Kunz J., 2017, *Phys. Rev. D*, 96, 064046
- Murata K., Soda J., 2006, *Phys. Rev. D*, 74, 044018
- Pani P., Loeb A., 2014, *J. Cosmology Astropart. Phys.*, 2014, 026
- Papanikolaou T., Vennin V., Langlois D., 2021, *J. Cosmology Astropart. Phys.*, 2021, 053
- Pearson J. M., Chamel N., Potekhin A. Y., Fantina A. F., Ducoin C., Dutta A. K., Goriely S., 2018, *MNRAS*, 481, 2994
- Pearson J. M., Chamel N., Potekhin A. Y., Fantina A. F., Ducoin C., Dutta A. K., Goriely S., 2019, *MNRAS*, 486, 768
- Ray A., Laha R., Muñoz J. B., Caputo R., 2021, *Phys. Rev. D*, 104, 023516
- Read J. I., 2014, *J. Phys. G: Nucl. Part. Phys.*, 41, 063101
- Ryde F., 1999, *Astrophys. Lett. Commun.*, 39, 281
- Ryde F., 2004, *ApJ*, 614, 827
- Saha A. K., Laha R., 2022, *Phys. Rev. D*, 105, 103026
- Sartore N., Ripamonti E., Treves A., Turolla R., 2010, *A&A*, 510, A23
- Smyth N., Profumo S., English S., Jeltema T., McKinnon K., Guhathakurta P., 2020, *Phys. Rev. D*, 101, 063005
- Sofue Y., 2020, *Galaxies*, 8, 37
- Wang S., Xia D.-M., Zhang X., Zhou S., Chang Z., 2021, *Phys. Rev. D*, 103, 043010

- Yazadjiev S. S., Doneva D. D., Popchev D., 2016, *Phys. Rev. D*, 93, 084038
- Zeldovich Y. B., Novikov I. D., 1967, *Soviet Ast.*, 10, 602

This paper has been typeset from a  $\text{\TeX}/\text{\LaTeX}$  file prepared by the author.